16TH EUROPEAN CONFERENCE ON EARTHQUAKE ENGINEERING THESSALONIKI 18 - 21 JUNE 2018

HYBRID BRIDGE BENT FOR ACCELERATED BRIDGE CONSTRUCTION USING POST-TENSIONED COLUMNS AND BRBS

Anurag UPADHYAY[1] and Chris P. PANTELIDES[2]

ABSTRACT

This paper investigates an innovative self-centering multi-column bridge bent system for Accelerated Bridge Construction (ABC) in seismic regions using finite-element modeling. The proposed design of the hybrid system consists of post-tensioned precast concrete columns in a two-column bridge bent equipped with one or two Buckling Restrained Braces (BRBs) as external supplementary energy dissipation devices. Two configurations of BRBs are considered: two BRBs in a chevron arrangement and one BRB in a diagonal arrangement. The BRB devices could be replaced after a severe earthquake whereas the gravity load bearing frame should remain undamaged. Large inelastic rotations are accommodated due to gap opening at the rocking planes without damage to the column concrete. Post-tensioned high-strength threaded steel bars, designed to stay elastic ensure self-centering of the columns. A numerical model of the bridge bent was subjected to quasi-static cyclic loading using OpenSees. Quasi-static cyclic analysis of the hybrid system was performed to optimize the ratio of BRB core area to post-tensioning steel area. Subsequently, the bridge structure was evaluated using nonlinear time history analyses using 22 far-field earthquake records from FEMA P695, scaled to the maximum credible earthquake level at the site. Fragility curves for the hybrid bridge bent show that it performed within the life safety limit performance state with less than 1.5% transient drift ratio and less than 0.5% residual drift ratio. Since damage was concentrated in the BRBs, the precast concrete frame remained mostly in the elastic range, and could be considered as operational.

Keywords: Bridge; Buckling Restrained Brace; Hybrid Design; Post-tensioning; Self Centering

1. INTRODUCTION

Post-tensioning is a commonly used method for building slender structures that can be constructed rapidly. Precast concrete bridge elements are included in the Accelerated Bridge Construction (ABC) method, which ensures minimum disturbance to commuters and residents at bridge construction sites. A new hybrid precast concrete bridge bent, capable of self-centering after seismic events and dissipating a sufficient amount of seismic input energy through external dampers (BRBs in this case) is proposed in this paper. Two configurations of BRB installation, a diagonal and a chevron arrangement are examined. The ratio of BRB core area to total post-tensioning steel area in the two columns (PT) is optimized through a parametric study. Both BRB arrangements are subjected to historical ground motions to assess the performance of the proposed design.

The concept of hybrid self-centering structural behavior originated from the stepping railway bridge over the South Rangitikei River in New Zealand (Cormack 1987), where rocking was combined with a hysteretic energy dissipation device. Similar features were provided for an industrial chimney at the Christchurch airport in New Zealand (Sharpe and Skinner 1983). The idea was then applied to concrete moment frame and coupled-wall buildings under the PREcast Seismic Structural Systems (PRESSS) program (MacRae and Priestley 1994; Stone et al. 1995; El-Sheikh et al. 1999; Kurama et al. 1999; Nakaki et al. 1999). Christopoulos et al. (2002) extended the concept to moment-resisting steel frames.

[1] PhD Student, Dept. of Civil and Environmental Engineering, University of Utah, Salt Lake City 84112. (email: anurag.upadhyay@utah.edu)
[2] Professor, Dept. of Civil and Environmental Engineering, University of Utah, Salt Lake City 84112.

Additional experimental work on self-centering structural walls was reported by Holden et al. (2003)., and Pérez et al. (2003). A number of analytical studies were carried out considering potential applications of self-centering to bridge columns (Kwan and Billington 2003a, b; Sakai and Mahin 2004; Heiber et al. 2005; Palermo et al. 2007). Ou et al. (2010) performed large-scale experiments on precast segmental post-tensioned bridge columns and showed that desired ductility and self-centering could be achieved. Shake table testing of cast-in-place hybrid concrete bridge columns was performed by Sakai et al. (2006). Marriott et al. (2009, 2011) carried out analytical studies and quasi-static cyclic tests on monolithic, purely rocking, and hybrid concrete columns, developing solutions for energy dissipation. Solberg et al. (2009) conducted quasi-static and pseudo-dynamic bidirectional tests on hybrid post-tensioned bridge columns with armored rocking interfaces. Guerrini (2015) conducted cyclic tests on post-tensioned precast concrete dual shell columns with external energy dissipation devices and successfully achieved self-centering up to a 3% drift ratio. These studies demonstrate that unbonded post-tensioning can be used to achieve self-centering of structures if yielding of post-tensioned bars could be prevented.

Previous numerical and experimental studies showed that BRB components in the bridge bent help the structure dissipate seismic energy, and improve the seismic performance of the bridge in the transverse direction (El-Bahey and Bruneau 2011, Bazaez and Dusicka 2016, Wang et al. 2016, Upadhyay and Pantelides 2017). BRBs have also been proposed to increase the seismic capacity of the bridge deck in the longitudinal direction (Celik and Bruneau 2009, Pantelides et al. 2016).

2. HYBRID SELF-CENTERING ENERGY DISSIPATING BRIDGE BENT CONCEPT

A self-centering energy dissipating hybrid precast concrete bridge bent design is proposed. The proposed bridge bent design, shown in Fig. 1, is a combination of a post-tensioned precast concrete bridge bent equipped with either two BRBs in a chevron arrangement, as shown in Fig. 1(a), or a single diagonal BRB, as shown in Fig. 1(b). Post-tensioning assists the structure in re-centering thus minimizing the residual drift ratio; BRBs dissipate hysteretic energy thus providing sufficient damping to the system to minimize damage to the precast concrete frame. The combination of post-tensioning in the precast concrete columns of the bridge bent and BRB hysteretic behavior leads to a "flag shaped" hysteresis curve. The concept is explained in Fig. 2 using backbone curves from nonlinear static pushover analysis. For design calculations, the behavior of both the BRBs and the post-tensioned (PT) precast concrete bridge bent is assumed to be bilinear. Due to post-tensioning, the initial lateral load capacity of the PT precast concrete bent starts from a non-zero lateral load depending on the area and initial post-tensioning stress of the PT bars. The BRB yield displacement is designed to be lower than the PT precast concrete bent yield displacement which ensures that the BRBs dissipate hysteretic energy while the bridge bent is still in the elastic region. The aim of the design is to ensure that the PT concrete bridge bent remains mostly elastic under seismic Maximum Credible Earthquake (MCE) level excitation and that it performs under the "operational" limit state while the BRBs dissipate sufficient hysteretic energy.

The analytical model of the bridge bent with post-tensioned precast concrete columns and the diagonal BRB arrangement is shown in Fig. 3. The post-tensioned columns were modeled with nonlinear beam-column elements using fiber elements and a section representing a column approximated with a circular cross-section. The main nodes of each column were located at the bottom of the foundation, the bottom, mid-height and top of the column, and the top of the cap beam. Slave nodes were used to anchor PT bars at the bottom of the foundation, the bottom and top of the column, and the top of the cap beam. End anchors of PT bars were modeled using rigid beam elements so that the nodes could move in a rigid plane. Interaction of PT bars and column during rocking was modeled using link elements with six degrees of freedom, which were free only in the vertical translation direction in order to simulate sliding between PT bar and grout inside the ducts. PT high-strength steel bars were modeled using the "Steel02" material model and "Corotational truss elements" in OpenSees (McKenna 2010).

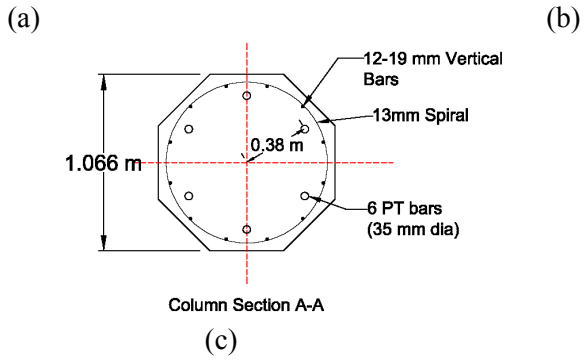

Figure 1. Proposed design of self-centering energy dissipating hybrid bent; (a) chevron, (b) diagonal arrangement; (c) column cross-section.

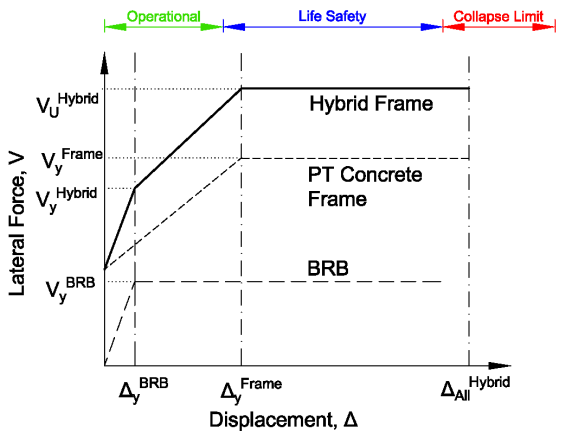

Figure 2. Concept of hybrid bent design.

The rocking behavior of the column was simulated by modeling a bed of zero length, uniaxial, compression-only springs at its base. The rocking plane was modeled with elastic rigid elements connecting the main and slave nodes. At the rocking plane, the gross column cross-section was discretized radially and circumferentially and springs were assigned inelastic material properties using the "concrete04" uniaxial material model. The cap beam was modeled with elastic beam-column elements. Initial post-tensioning in the PT bars was simulated using the "InitialStress" command and an equivalent vertical load was assigned at the top node of the PT bar anchor simulating the post-tensioning force. The diagonal BRB was modeled with "twoNodeLink" elements in OpenSees connected as shown in Fig. 3. The "Steel02" model (Giuffré-Menegotto-Pinto material with isotropic strain hardening) was used to simulate BRB hysteretic behavior.

3. PARAMETRIC STUDY

A parametric study was performed to optimize the BRB steel core area of the hybrid bridge bent. The ratio of BRB steel core area to the total PT high-strength steel area in the two columns, referred to as "*Area Ratio (ρ)*" was selected as the variable. Both BRB schemes (Fig. 1) were subjected to quasi-static cyclic loading by varying ρ. The BRBs were assumed to fail at a 3.5% tensile strain which generally equals to the air gap to BRB core yielding length ratio with a manufactured air gap limit of 75-100 mm (Andrews et al. 2009, Xu and Pantelides 2017). For the chevron arrangement of BRBs in Fig. 1(a), the total steel core area of the external dampers was divided equally between the two BRBs. Table 1 shows the BRB steel core area for each case. The self-centering capability was quantified through the relative self-centering efficiency (RSE) index, defined by Sideris et al. as (2014):

$$\text{RSE} = 1 - \frac{u^{+}_{res} - u^{-}_{res}}{u^{+}_{peak} - u^{-}_{peak}} \quad (1)$$

where u^{+}_{res} and u^{+}_{res} = positive and negative residual displacements, respectively. Figure 4 shows a comparison of the cyclic hysteresis of hybrid systems for various values of ρ. It is evident that the hysteretic energy dissipated by the diagonal BRB arrangement is greater than the chevron BRB arrangement. The peak base shear resisted by the diagonal BRB arrangement is higher than the chevron BRB arrangement for the same ρ. This is because the angle of the BRB from the horizontal in the diagonal case is smaller than the angle in the chevron BRB arrangement. Figure 5(a) shows the cyclic hysteresis for ρ =50% for the chevron BRB arrangement. The hybrid system dissipated hysteretic energy while the PT concrete frame remained mostly elastic. The BRB reached the 3.5% tensile failure strain at a 3.6% drift ratio leading to a sudden decrease in load carrying capacity of the system.

The residual drift ratio (drift at zero lateral force) in the chevron BRB arrangement was found to be much less than the diagonal BRB arrangement. The residual drift ratio increases with ρ as demonstrated in Fig. 4. For a larger BRB core area, a higher PT force is required to overcome the plastic deformation of the BRB steel core; the BRB contribution dominates, thus increasing the residual drift

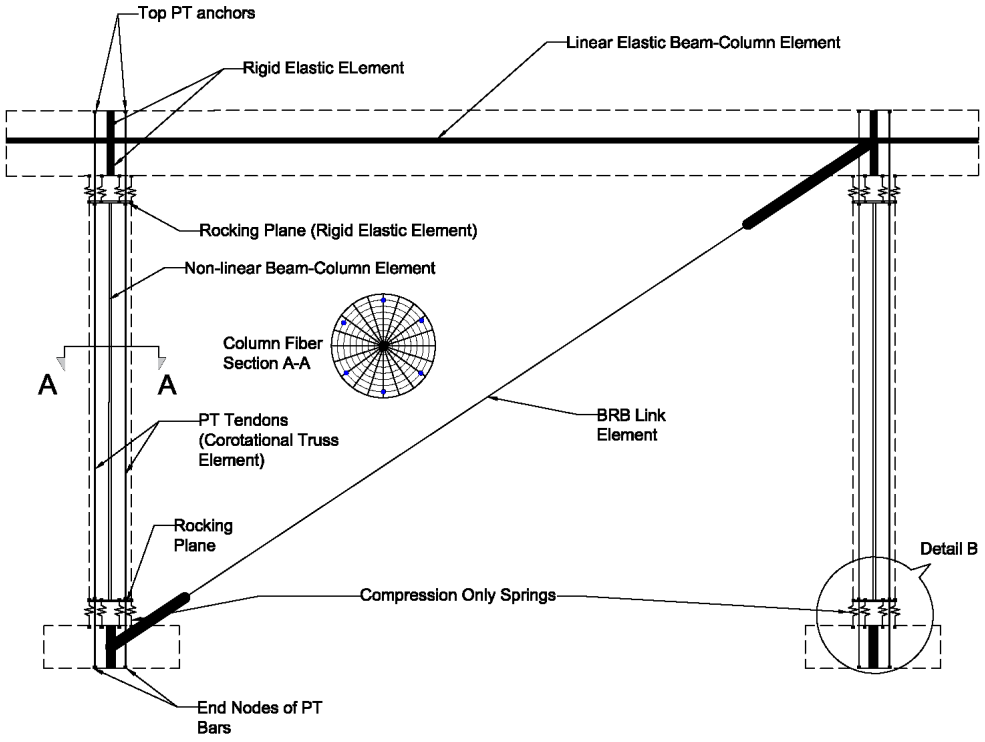

Figure 3. Analytical model of proposed hybrid bridge bent with diagonal BRB arrangement.

Table 1. BRB core area and length for parametric study.

	Diagonal	Chevron	
		BRB1	BRB2
	Core Length (m)		
	5.21	3.79	3.79
ρ (%)	Core Area (mm^2)		
12.5	1529	765	765
17.5	2141	1070	1070
25.0	3058	1529	529
32.5	3975	1988	1988
37.5	4587	2294	2294
50.0	6116	3058	3058

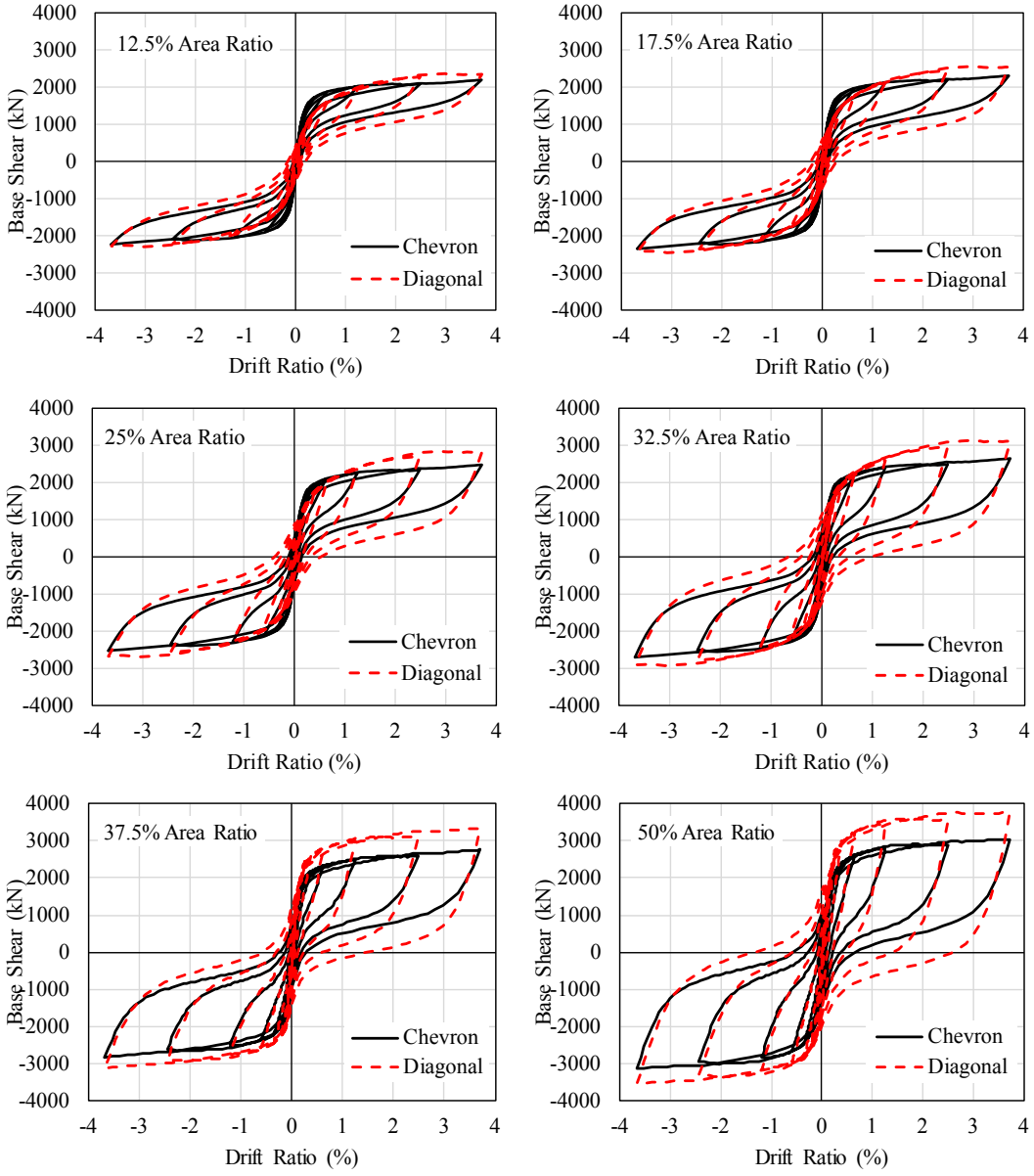

Figure. 4 Cyclic hysteresis for various cases of *Area Ratio* (ρ) in the parametric study.

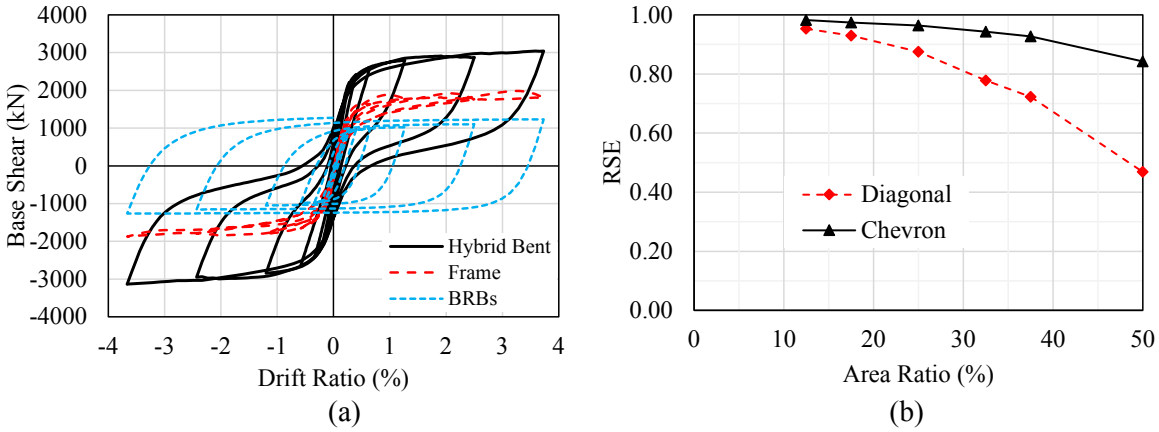

Figure 5. Cyclic performance of hybrid bent; (a) force shared by precast concrete frame and BRBs in the chevron arrangement for ρ = *50%*; (b) relative self-centering efficiency between diagonal and chevron arrangement for various hybrid bridge bent systems.

ratio of the system. RSE values for various cases in the parametric study (Table 1) are shown in Fig. 5(b). A value of RSE = 1 implies a perfect self-centering system. The system with ρ = 12.5% achieved the maximum RSE of 0.98 for the chevron arrangement and a maximum RSE of 0.95 for the diagonal arrangement. For ρ = 50% the chevron scheme reached a RSE = 0.84 while the diagonal arrangement reached a RSE = 0.47.

4. COMPARISON OF HYBRID BRIDGE BENT WITH MONOLITHIC CAST-IN-PLACE BRIDGE BENT

The performance of the hybrid self-centering precast concrete bridge bent was compared to a cast-in-place (CIP) monolithic concrete bridge bent with dimensions similar to the bent shown in Fig. 1. The longitudinal reinforcement ratio was selected to be 1% which is the minimum required according to AASHTO LRFD (2012) Bridge Design Specifications. The CIP columns were reinforced longitudinally with 15#9 (25 mm dia.) bars and transversely with #4 (13 mm dia.) spirals at 51 mm pitch throughout the column height. The axial load index, which is the ratio of the axial load to the product of column area and column compressive strength was assumed as 10%. The CIP bent was designed in such a way that it had a peak lateral load strength equivalent to the hybrid bent. Fig. 6(a) shows the cyclic hysteresis comparison of the CIP and hybrid bent with ρ =50% and chevron BRB scheme. It is evident that the CIP bent dissipates much more energy than the hybrid bent due to yielding of the column steel bars crossing the column-foundation and column-cap beam interface. The hysteretic loops of the hybrid bent were significantly different from those of the CIP, exhibiting a flag-shaped response because of the use of post-tensioning bars and BRBs. The stiffness of the hybrid bent was lower than that of the CIP bent because of the larger number of bars in the CIP columns. RSE values were calculated for both bridge bent types to compare re-centering capability (Fig. 6 b). The CIP bent showed higher self-centering in the first cycle as compared to the hybrid bent. This is because the bents were still in the elastic region and the stiffness of the CIP bent was higher than that of the hybrid bent. For subsequent cycles, the RSE values for the CIP bent were reduced significantly while the self-centering capability of the hybrid bent increased. The relative self-centering efficiency in the 5th cycle (4% drift ratio) was 0.20 for the CIP bent and 0.90 for the hybrid bent. It is obvious from the analysis that the hybrid bent has a better self-centering capacity.

5. NONLINEAR TIME HISTORY ANALYSIS

Nonlinear time history analysis was performed for the hybrid bent with the Chevron arrangement and

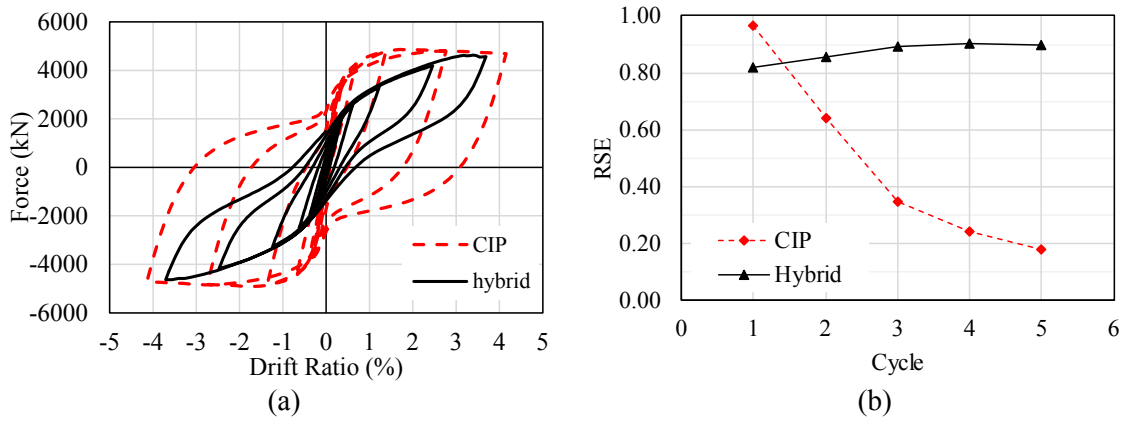

Figure 6. Comparison of cyclic performance of CIP and hybrid bent: (a) Hysteresis; (b) RSE values for each cycle.

ρ = 50% to assess its performance in historic earthquakes. The hybrid bent had a fundamental period of T_1 = 0.31s which corresponds to a Maximum Considered Earthquake (MCE) spectral acceleration equal to Sa = 1.48g for a Salt Lake City, Utah site with soil type D. The Kobe (1995), Shin-Osaka station, ground acceleration scaled to two levels, the MCE with S_a = 1.48g and for an earthquake with Sa = 2.0g was used to analyze the structure. Performance limits were adopted from the Vision 2000 document (SEAOC 1995). The response of the bridge bent remained mostly elastic for ground motions scaled to the Design Basis Earthquake (DBE) level and showed a flag shaped hysteresis for the MCE level. The peak drift ratio exceeded the near collapse limit (2.5% drift ratio) for the ground motion scaled to Sa = 2.0g, as shown in Fig. 7(a). During small ground motion pulses, the column elastic stiffness was effective thus keeping the hysteresis curve close to the initial stiffness of the structure. Once activation of the post-tensioning force in the PT bars was initiated, the hysteresis curve moved along the second stiffness of the system. Larger cyclic displacements caused increased BRB forces, leading to the flag shaped hysteresis of the hybrid system. The peak strain in the PT bars was 0.38% and the peak core concrete compressive strain was 0.3%. The peak strain demand in the BRB core was 2.95%, which is below the assumed tensile failure strain. The BRB dissipated most of the seismic input energy while the PT frame remained mostly elastic as observed previously (Fig. 5(a)).

Fragility curves (or cumulative distribution functions, CDFs) were developed based on analysis of a set of 22 far-field ground motions, as recommended in FEMA P695 (FEMA 2009) and scaled to the site MCE level. Fig. 7(b) presents CDFs for the peak and residual drift ratios of the hybrid bent with the chevron arrangement and ρ = 50%. The peak drift ratio of the hybrid bridge bent was always below the life safety limit of 1.5% but exceeded the operational limit of 0.5% for 90% of the cases. The residual drift ratio was below 0.2% for 90% of the cases. The residual drift ratio can be assumed to be negligible. Since the predicted damage was concentrated in the BRBs and the precast concrete frame remained mostly in the elastic range, the precast concrete load bearing frame can be considered as “operational” while the entire structural system performed within the “life safety” limit state.

6. CONCLUSIONS

A self-centering energy dissipating hybrid precast concrete bridge bent system is proposed using post-tensioned precast concrete columns in a two-column bridge bent equipped with BRBs. Three-dimensional numerical models of the hybrid bridge bent are developed with two different BRB arrangements, chevron and diagonal. A parametric study is performed to compare the self-centering capability of the bridge bent with the two BRB schemes and various ratios of total BRB steel core area to total PT high-strength steel area in the columns. Fragility curves are developed for the hybrid precast concrete bridge bent using 22 far-field earthquake ground motions scaled to the Maximum Credible Earthquake level. The following conclusions and findings are obtained on the basis of the results of the

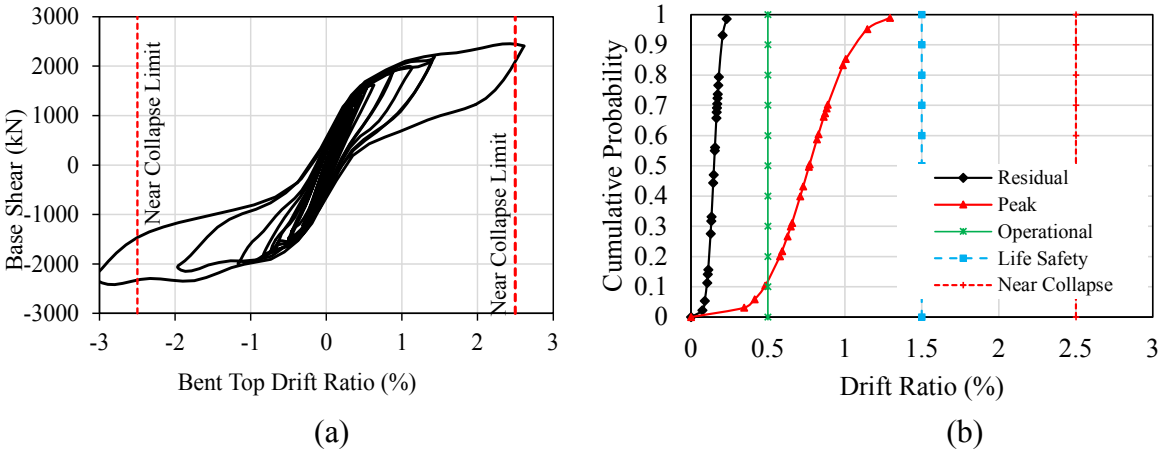

Figure 7. Performance of hybrid bridge bent with ρ = 50%: (a) for Kobe (1995) ground motion scaled to S_a = 2.0g; (b) fragility curves using 22 far-field ground motions scaled to MCE.

numerical analysis:

1. Cyclic analysis of the hybrid bent shows that post-tensioned bars were effective for re-centering while BRBs dissipated the bulk of the hysteretic energy. The hybrid system achieved significant displacement ductility due to BRB yielding while the PT high-strength steel bars remained elastic.
2. The hybrid bent with the chevron arrangement of BRBs achieved higher re-centering but a smaller energy dissipation compared to the diagonal arrangement for the same area ratio (ρ). With an increase in BRB core area, re-centering capability decreases; for a ρ =50%, the relative self-centering efficiency of the chevron and diagonal arrangements was 84% and 47%, respectively.
3. A fragility analysis for 22 far-field ground motions, as recommended in FEMA P695, scaled to the site MCE level was performed. Fragility curves for the hybrid bridge bent show that it performed within the life safety limit state with less than 1.5% transient drift ratio and less than 0.5% residual drift ratio.
4. Based on damage assessment of the structure, the PT precast concrete load bearing frame remained in the elastic range and suffered negligible structural damage since all the damage was concentrated in the BRBs; thus it could be considered as operational.

7. ACKNOWLEDGMENTS

The authors would like to acknowledge the financial support of the Mountain Plains Consortium under contract MPC-491.

8. REFERENCES

AASHTO., (2012). *AASHTO LRFD bridge design specifications, 6th Ed*. American Association of State Highway and Transportation Officials, Washington, DC.

Andrews, B., Fahnestock, L., and Song, J. (2009). Ductility capacity models for buckling-restrained braces. *Journal of Construction Steel Research*, 65(8), 17112-1720.

Bazaez, R., and Duscika, P. (2016). Cyclic behavior of reinforced concrete bridge bent retrofitted with Buckling restrained braces. *Engineering Structures*, 119, 34-48.

Celik, O., and Bruneau, M. (2009). Seismic behavior of bidirectional resistant ductile end diaphragms with buckling restrained braces in straight steel bridges. *Engineering Structures*, 31(2), 380-393.

Christopoulos, C., Filiatrault, A., Uang, C.-M., and Folz, B. (2002). Post-tensioned energy dissipating connections for moment resisting steel frames. *J. Struct. Eng*., 128(9), 1111–1120.

Cormack, L. G. (1987). The Design and Construction of Major Bridges on the Mangaweka Rail Deviation. *IPENZ Annual Conference*, Christchurch, May 10-14, 1987, 1-14.

El-Bahey, S., and Bruneau, M. (2011). Buckling restrained braces as structural fuses for the seismic retrofit of reinforced concrete bridge bents. *Engineering Structures*, 33(3), 1052-1061.

El-Sheikh, M. T., Sause, R., Pessiki, S., and Lu, L.-W. (1999). Seismic behaviour and design of unbonded post-tensioned precast concrete frames. *PCI J*., 44(3), 54–71.

FEMA (2009). *Quantification of Building Seismic Performance Factors*. Applied Technology Council (ATC-63 project). Federal Emergency Management Agency, Washington, DC.

Guerrini, G., Restrepo, J. I., Massari, M. A., and Vervelidis, A. (2015). Seismic behavior of post-tensioned self-centering precast concrete dual-shell steel columns. *J. Structural Eng.*, 141(4), 04014115.

Heiber, D. G., Wacker, J. M., Eberhard, M. O., and Stanton, J. F. (2005). *Precast concrete pier systems for rapid construction of bridges in seismic regions.* Rep. No. WA-RD 611.1, Washington Dept. of Transportation, Olympia, WA.

Holden, T., Restrepo, J. I., and Mander, J. B. (2003). Seismic performance of precast reinforced and prestressed concrete walls. *J. Struct. Eng*., 129(3), 286–296.

Kurama, Y., Sause, R., Pessiki, S., and Lu, L. W. (1999). Lateral load behavior and seismic design of unbonded post-tensioned precast concrete walls. *ACI Struct. J*., 96(4), 622–632.

Kwan, W. P., and Billington, S. (2003a). Unbonded posttensioned concrete bridge piers. I: Monotonic and cyclic analyses. *J. Bridge Eng*., 8(2), 92–101.

Kwan, W. P., and Billington, S. (2003b). Unbonded posttensioned concrete bridge piers. II: Seismic analyses. *J. Bridge Eng*., 8(2), 102–111.

MacRae, G. A., and Priestley, M. J. N. (1994). *Precast post-tensioned ungrouted concrete beam-column subassemblage tests.* Rep. No. SSRP-94/10, Dept. of Applied Mechanics and Eng. Sciences, Univ. of California at San Diego, La Jolla, CA.

Marriott, D., Pampanin, S., and Palermo, A. (2009). Quasi-static and pseudo-dynamic testing of unbonded post-tensioned rocking bridge piers with external replaceable dissipaters. *Earthquake Eng. Struct. Dyn*., 38(3), 331–354.

Marriott, D., Pampanin, S., and Palermo, A. (2011). Biaxial testing of unbonded post-tensioned rocking bridge piers with external replaceable dissipaters. *Earthquake Eng. Struct. Dyn*., 40(15), 1723–1741.

Nakaki, S. D., Stanton, J. F., and Sritharan, S. (1999). An overview of the PRESSS five-story precast test building. *PCI J*., 44(2), 26–39.

Ou, Y.-C., Wang, P.-H., Tsai, M.-S., Chang, K.-C., and Lee, G. C. (2010). Large-scale experimental study of precast segmental unbonded posttensioned concrete bridge columns for seismic regions. *J. Struct. Eng*., 136(3), 255–264.

Palermo, A., Pampanin, S., and Marriott, D. (2007). Design, modeling, and experimental response of seismic resistant bridge piers with posttensioned dissipating connections. *J. Struct. Eng*., 133(11), 1648–1661.

Pantelides, C., Ibarra, L., Wang, Y., and Upadhyay, A. (2016). *Seismic rehabilitation of skewed and curved bridges using a new generation of buckling restrained braces.* Report No. MPC 16-315, Fargo, ND.

Pérez, F. J., Pessiki, S., Sause, R., and Lu, L.-W. (2003). Lateral load tests of unbonded post-tensioned precast concrete walls. *Special Publication of Large-Scale Structural Testing*, *ACI*, SP 211(8), 161–182.

Sakai, J., and Mahin, S. A. (2004). *Analytical investigations of new methods for reducing residual displacements of reinforced concrete bridge columns.* Rep. No. PEER 2004/02, Pacific Earthquake Engineering Research Center, Berkeley, CA.

Sakai, J., Jeong, H., and Mahin, S. A. (2006). Reinforced concrete bridge columns that recenter following earthquakes." *Proc., 8th U.S. National Conf. on Earthquake Engineering*, Paper No. 1421, Earthquake Engineering Research Institute, Oakland, CA.

SEAOC. (1995). *Vision 2000: Performance-Based Seismic Engineering of Buildings*. Structural Engineers Association of California, Sacramento, CA.

Sharpe, R. D., and Skinner, R. I. (1983). The seismic design of an industrial chimney with rocking base. *Bulletin of the New Zealand National Society for Earthquake Engineering* 1983; 16(2): 98-106.

Sideris, P., Aref, A. J., and Filiatrault, A. (2014). Quasi-static cyclic testing of a large-scale hybrid sliding-rocking segmental column with slip-dominant joints. *J. Bridge Eng.*, 19(10), 04014036:1-11.

Solberg, K., Mashiko, N., Mander, J. B., and Dhakal, R. P. (2009). Performance of a damage-protected highway bridge pier subjected to bidirectional earthquake attack. *J. Struct. Eng.*, 135(5), 469–478.

Stone, W. C., Cheok, G. S., and Stanton, J. F. (1995). Performance of hybrid moment-resisting precast beam-column concrete connections subjected to cyclic loading. *ACI Struct. J.*, 91(2), 229–249.

Upadhyay, A., and Pantelides, C. (2017). Comparison of the seismic retrofit of a three-column bridge bent with buckling restrained braces and self centering braces. *Proc. of the Structural Congress 2017*, Denver, CO.

Wang, Y., Ibarra, L., and Pantelides, C. (2016). Seismic retrofit of a three-span RC bridge with buckling-restrained braces. *J. of Bridge Eng.*, 21(11):04016073.

Xu, W. and Pantelides, C. (2017). Strong-axis and weak-axis buckling and local bulging of buckling-restrained braces with prismatic core plates. *Engineering Structures*, 153, 279-289.